Single Turnover Reveals Oxygenated Intermediates in Toluene/o-Xylene Monooxygenase in the Presence of the Native Redox Partners

HHS Public Access

Author manuscript

J Am Chem Soc. Author manuscript; available in PMC 2015 December 02.

Published in final edited form as:

J Am Chem Soc. 2015 August 26; 137(33): 10520–10523. doi:10.1021/jacs.5b07055.

Single Turnover Reveals Oxygenated Intermediates in Toluene/o-Xylene Monooxygenase in the Presence of the Native Redox Partners

Alexandria Deliz Liang and **Stephen J. Lippard**

Department of Chemistry, Massachusetts Institute of Technology, Cambridge, Massachusetts, 02139, United States

Abstract

Toluene/*o*-xylene monooxygenase (ToMO) is a non-heme diiron protein that activates O_2 for subsequent arene oxidation. ToMO utilizes four protein components, a catalytic hydroxylase (ToMOH), a regulatory protein (To-MOD), a Rieske protein (ToMOC), and a reductase (ToMOF). Here, we examine O_2 activation and substrate hydroxylation in the presence of all four-protein components. Studies of this system demonstrate the importance of ToMOC for formation of the active hydroxylating species that are not revealed when dithionite and mediators are used as the reductant. This reactivity is discussed in light of other O_2-activating, non-heme diiron enzymes.

O_2 activation by non-heme diiron enzymes generates reactive intermediates capable of hydrocarbon hydroxylation, epoxidation, desaturation, and radical formation.[1] Because structurally similar active sites catalyze diverse chemical transformations, the mechanisms by which these diiron enzymes control reactivity are of particular interest.

Toluene/*o*-xylene monooxygenase (ToMO) belongs to a family of diiron proteins termed bacterial multicomponent monooxygenases (BMMs) that activate O_2 to oxidize hydrocarbon substrates (Scheme 1).[2]

ToMO catalyzes the hydroxylation of toluene to form *o*-, *m*-, and *p*-cresol, and can also perform the catalytic, regiospecific hydroxylation of phenol to form catechol.[3] Four protein components are required to carry out efficient catalysis, a dimeric hydroxylase (ToMOH), a regulatory protein (ToMOD), a reductase (ToMOF), and a Rieske protein (ToMOC).[2a] Previous O_2-activation studies with ToMO utilized a simplified protein system comprising ToMOH, ToMOD, and sodium dithionite as reductant with and methyl viologen (2e-MV) as an electron-transfer mediator.[4] In these earlier experiments, a colorless intermediate termed $ToMOH_{peroxo}$ was generated.[4a] Here, we sought to determine whether single turnover by the

*Corresponding Author*lippard@mit.edu.

ASSOCIATED CONTENT

Supporting Information. Experimental details, Figures S1–S9, and Tables S1–S3. This material is available free of charge via the Internet at http://pubs.acs.org.

No competing financial interests have been declared.

native system, $ToMO_{red}$ (ToMOH, ToMOD, ToMOC, ToMOF, and NADH) differs from that observed using 2e-MV to reduce ToMOH.

Under single turnover conditions with limiting [NADH], the rate of phenol hydroxylation to form catechol by $ToMO_{red}$ and O_2 depends on the ratio of ToMOC per diiron sites of ToMOH, hereafter ToMOC:diiron (Figure 1).

Using 0.01ToMOC:diiron, 36(3)% of the diiron sites form catechol by 2 s with a rate constant of 8(1) s^{-1}. A slow increase in product formation follows (Figure S1). After 10 min, 84(4)% of the diiron sites produce catechol. In contrast, using 1ToMOC:diiron, 70(4)% of the diiron sites produce catechol by 2 s. The product yields after 10 min are similar in both reactions. These results suggest that two phases of product formation occur, a fast phase and a slow phase. Inclusion of stoichiometric ToMOC promotes product formation by increasing the amount of product formed in the fast phase. Importantly, the rate constant of each phase is not significantly affected by ToMOC concentration, demonstrating that ToMOC does not directly participate in substrate hydroxylation.

In these single-turnover experiments, pre-incubation of NADH and the protein components of ToMO pre-forms the reduced hydroxylase, and product quantification requires rapid protein precipitation, which releases product bound at the active site. Thus, ToMOC must influence steps(s) between reduction of the diiron site and product release. These steps would include O_2 activation, aromatic substrate binding, substrate hydroxylation, and any conformational changes necessary for the initiation of each step.

In the presence of 0.01ToMOC:diiron, O_2 activation by $ToMO_{red}$ yields rapid absorbance changes at 420 and 675 nm (Figure 2), which are not observed when 2e-MV is used as the reductant.[4a] Because ToMOC contains a redoxdependent chromophore, higher ratios of ToMOC:diiron were not suitable for monitoring absorbance changes caused by the diiron center.[§] These absorbance changes are absent when either hydroxylase or O_2 is omitted (Figure S2), strongly indicating that the features result from reaction of O_2 with the hydroxylase.

When the concentration of O_2 was varied between 375 and 625 μM, the observed kinetics were unchanged (Figure S3 and Table S1), indicating that the interaction of ToMOH with O_2 must be faster than the first observable step, as found for related diiron enzymes.[5] The simplest interpretation of these data invokes the formation of four species: 675A, $t_{max} \leq 2$ ms, k_{decay} = 40(5) s^{-1}; 420A, t_{max} = 200 ms, $k_{formation}$ = 23(1) s^{-1}; 420B, $t_{max} \sim 70$ s, $k_{formation}$ 0.023(2) s^{-1}; and H_{ox}, $t_{max} > 1000$ s, $k_{formation}$ 0.0018(2) s^{-1}.

The maximum accumulation of 675A occurs before the mixing time of the instrument, 2 ms, which limits the ability to fully characterize this species by rapid mixing techniques. Intermediates 420A and 420B were characterized by rapid freeze-quench (RFQ) Mössbauer

[§]Under these conditions, the maximum absorbance change for redox cycling of ToMOC and ToMOF is 3 mAU at 420 nm and 0.25 mAU at 675 nm.

spectroscopy.† RFQ Mössbauer reactions were conducted at 0.1ToMOC:diiron and 1ToMOC:diiron. Both sample conditions yielded similar Mössbauer parameters (Figure S4).

Species 420A accumulates with a rate constant similar to that observed for $ToMOH_{peroxo}$ (~26 s^{-1}), the colorless intermediate previously reported when 2e-MV was used to reduce ToMOH.[4a] For a sample frozen after 0.2 s, approximately 80% of the iron sites are iron(III) with Mössbauer parameters δ = 0.54 mm/s and ΔE_Q = 0.67 mm/s (Figure 2). These Mössbauer parameters are identical to those reported for $ToMOH_{peroxo}$.[4a] The remaining 20% is iron(II) with Mössbauer parameters δ = 1.31 mm/s and ΔE_Q = 2.88 mm/s, corresponding to unreacted diiron(II).[4a,6] 420A is stable for > 6 s. Because of its long lifetime, we initially questioned whether this species is a diiron-O_2 intermediate. Diiron-O_2 adducts with lifetimes from 3 s to 3 h have been reported, however.[7]

Given the significant difference in the absorption profiles of 420A (Figure S5) and $ToMOH_{peroxo}$, these intermediates must be different. Altering the reaction pH did not quench the absorbance corresponding to 420A (Figure S6), demonstrating that excess protons alone cannot induce formation of $ToMOH_{peroxo}$ rather than 420A. Thus, other changes must be required, such as a conformational change.

Generation of 420B and formation of H_{ox} occurs with rate constants significantly smaller than steady-state turnover (toluene hydroxylation, ~0.5 s^{-1}),[9] suggesting that these steps are not relevant to catalysis. Analysis of intermediate 420B is provided in the Supporting Information. The final species has negligible absorbance at 420 and 675 nm, consistent with the diiron(III) resting state, H_{ox}.

The absorbance changes were also monitored in the presence of excess toluene (Figure 3). The decay of the first species, 675A, is unaffected by toluene, indicating that this species is not responsible for oxidizing aromatic substrates. In contrast, addition of toluene significantly alters the absorbance changes at 420 nm.

The absorbance changes at 420 nm are well described by an A–>B–>C–> D model with rate constants of 40(5) s^{-1}, 15(3) s^{-1}, and 0.61(4) s^{-1}. Based on the wavelength of maximum absorbance, rate of formation, and Mössbauer parameters, we assign the first species to intermediate 420A. The decay of 420A occurs rapidly in the presence of substrate (15 s^{-1}), consistent with 420A being responsible for substrate oxidation. Instead of forming H_{ox} directly, 420A decays to generate a species with t_{max} ~ 0.5 s (420-Ar), corresponding to toluene oxidation. Species 420-Ar is not observed in the absence of substrate and absorbs at both 420 and 675 nm. The formation rate constant of 420-Ar is similar to that observed for hydroxylation of phenol in our single-turnover experiments above. Binding of phenolic derivatives to the diiron active site increases the absorbance at 420 and 675 nm (Figure S7). Based on these observations, we assign 420-Ar to a cresol-diiron adduct resulting from hydroxylation of toluene.

†Only ToMOH was enriched with ^{57}Fe. The natural abundance of ^{57}Fe is 2%;[14] therefore the spectra result exclusively from the iron atoms of ToMOH.

In the final phase, 420-Ar decays with a rate constant of 0.61 s^{-1}, and the absorbance at 420 and 675 nm decreases. These changes are consistent with product release from the active site. The rate constant associated with this step is much smaller than that observed in our single-turnover experiments but is similar to the rate of steady-state turnover.[9] Thus, release of product may be rate limiting for steady-state turnover, as previously proposed for the analogous BMM toluene 4-monooxygenase (T4MO) based on X-ray crystallographic data.[10] O_2 activation in the presence of phenol was also examined, but proved to be much more complex than that observed with toluene (Figure S8). The increased complexity in the presence of phenol probably results from formation of both diiron-phenol and diiron-catechol adducts during single turnover.

Three important conclusions are evident from this work: (i) ToMOC is critical for formation of an active hydroxylating species, (ii) in the presence of ToMOC a previous undetected intermediate, 420A, is responsible for substrate hydroxylation, (iii) ToMOH is capable of greater than half-sites reactivity. Our conclusions are discussed below in light of previous work and other diiron proteins.

The difference in reactivity between the natural system and the 2e-MV simulation is surprising, given that the BMM soluble methane monooxygenase (sMMO) undergoes single turnover very well using 2e-MV as the reduction system.[11] A comparison of the absorbance changes observed for ToMO and sMMO are provided in Figure S9. For the multicomponent, non-heme diiron protein stearoyl-acyl carrier protein desaturase (Δ9D), an inactive peroxo species forms when the diiron reducing protein is replaced with sodium dithionite.[12] The chemical or physical changes that contribute to promotion of activity by the ferredoxin of Δ9D remain unknown. For toluene monooxygenases, however, a recent X-ray structure of the hydroxylase and Rieske protein complex for T4MO hints at a possible mechanism for Rieske protein function. In the 2.05-Å structure of the complex, residue E104 adopts a different conformation than those previously reported for BMMs (Figure 4).[13]

Movement of E104 alters hydrogen bonding at the active site.[13] Computational analyses of peroxo intermediates formed at carboxylate-bridged diiron centers indicate that the transition near 420 nm corresponds to LMCT from both the carboxylate and the peroxo ligand at the diiron site, and that these transitions are sensitive to the carboxylate orientation.[8] Thus, the differing absorbance features between the 2e-MV reduced system and the Rieske protein reduced system may arise from conformational changes of E104, a difference in the peroxo ligand coordination, or alteration of the hydrogen-bonding network near the active site.

The structure of the newly discovered intermediate 420A may correspond to any one of many (hydro)peroxo-diiron conformations. Because 420A is long-lived and has Mössbauer properties similar to those observed and calculated for μ-1,2-peroxodiiron intermediates,[8] we tentatively assign 420A as such a species.

Previous O_2-activation experiments reported half-sites reactivity with respect to the hydroxylase dimer.[4a,4d] The current work shows greater than 50% reactivity. This difference in activity may be a result of includng ToMOC or of the ratio of O_2 to ToMOH used in our

experiments. Here, 1.25 equivalents of O_2 per diiron sites are present, whereas in previous Mössbauer studies[4a,4d] we estimate that the ratio was ~ 0.6, based on the O_2 saturation limit.

In summary, we demonstrate the importance of the natural reduction component for efficient hydroxylation and O_2 activation by the multicomponent diiron protein, ToMO. Using this knowledge, we were able to identify a previously unobserved species, 420A, during O_2 activation by the diiron protein ToMO. A proposed scheme to account for the observed O_2-activation kinetics is given in Figure 4B. Further insight into the effects of ToMOC at a molecular level would benefit from high-resolution structural data of the oxidized and reduced systems.

Supplementary Material

Refer to Web version on PubMed Central for supplementary material.

ACKNOWLEDGMENT

The authors would like to acknowledge Tsai-Te Lu and Woon Ju Song for helpful discussions.

Funding Sources

This work was supported by NIH Grant GM032134 from the National Institute of General Medical Sciences (NIGMS). ADL was supported in part by the NIH NIGMS Biotechnology Training Program Grant T32 GM008334.

REFERENCES

1. Kurtz, DM.; Boice, E.; Caranto, JD.; Frederick, RE.; Masitas, CA.; Miner, KD. Encyclopedia of Inorganic and Bioinorganic Chemistry. John Wiley & Sons, Ltd; 2011.
2. (a) Cafaro V, Scognamiglio R, Viggiani A, Izzo V, Passaro I, Notomista E, Dal Piaz F, Amoresano A, Casbarra A, Pucci P, Di Donato A. Eur. J. Biochem. 2002; 269:5689. [PubMed: 12423369] (b) Leahy JG, Batchelor PJ, Morcomb SM. Fems Microbiol Rev. 2003; 27:449. [PubMed: 14550940]
3. Cafaro V, Notomista E, Capasso P, Di Donato A. Appl Environ Microb. 2005; 71:4736.
4. (a) Murray LJ, Naik SG, Ortillo DO, Garcia-Serres R, Lee JK, Huynh BH, Lippard SJ. J. Am. Chem. Soc. 2007; 129:14500. [PubMed: 17967027] (b) Song WJ, Behan RK, Naik SG, Huynh BH, Lippard SJ. J. Am. Chem. Soc. 2009; 131:6074. [PubMed: 19354250] (c) Song WJ, Gucinski G, Sazinsky MH, Lippard SJP. Natl Acad Sci USA. 2011; 108:14795.(d) Song WJ, Lippard SJ. Biochemistry. 2011; 50:5391. [PubMed: 21595439] (e) Song WJ, McCormick MS, Behan RK, Sazinsky MH, Jiang W, Lin J, Krebs C, Lippard SJ. J. Am. Chem. Soc. 2010; 132:13582. [PubMed: 20839885]
5. Stahl SS, Francisco WA, Merkx M, Klinman JP, Lippard SJ. J. Biol. Chem. 2001; 276:4549. [PubMed: 11073959]
6. Pikus JD, Studts JM, Achim C, Kauffmann KE, Münck E, Steffan RJ, McClay K, Fox BG. Biochemistry. 1996; 35:9106. [PubMed: 8703915]
7. (a) Vu VV, Emerson JP, Martinho M, Kim YS, Münck E, Park MH, Que L. P Natl Acad Sci USA. 2009; 106:14814.(b) Banerjee R, Meier KK, Münck E, Lipscomb JD. Biochemistry. 2013; 52:4331. [PubMed: 23718184] (c) Tinberg CE, Lippard SJ. Biochemistry. 2009; 48:12145. [PubMed: 19921958]
8. (a) Jensen KP, Bell CB, Clay MD, Solomon EI. J. Am. Chem. Soc. 2009; 131:12155. [PubMed: 19663382] (b) Srnec M, Rokob TA, Schwartz JK, Kwak Y, Rulíšek L, Solomon EI. Inorg Chem. 2012; 51:2806. [PubMed: 22332845]
9. Liang AD, Lippard SJ. Biochemistry. 2014; 53:7368. [PubMed: 25402597]

10. Bailey LJ, Acheson JF, McCoy JG, Elsen NL, Phillips GN, Fox BG. Biochemistry. 2012; 51:1101. [PubMed: 22264099]

11. (a) Liu Y, Nesheim JC, Paulsen KE, Stankovich MT, Lipscomb JD. Biochemistry. 1997; 36:5223. [PubMed: 9136884] (b) Valentine AM, Stahl SS, Lippard SJ. J. Am. Chem. Soc. 1999; 121:3876.

12. (a) Broadwater JA, Ai JY, Loehr TM, Sanders-Loehr J, Fox BG. Biochemistry. 1998; 37:14664. [PubMed: 9778341] (b) Sobrado P, Lyle KS, Kaul SP, Turco MM, Arabshahi I, Marwah A, Fox BG. Biochemistry. 2006; 45:4848. [PubMed: 16605252]

13. Acheson JF, Bailey LJ, Elsen NL, Fox BG. Nature Communications. 2014; 5

14. Drago, RS.; Drago, RS. Physical Methods for Chemists. 2nd ed.. Ft. Worth: Saunders College Pub.; 1992.

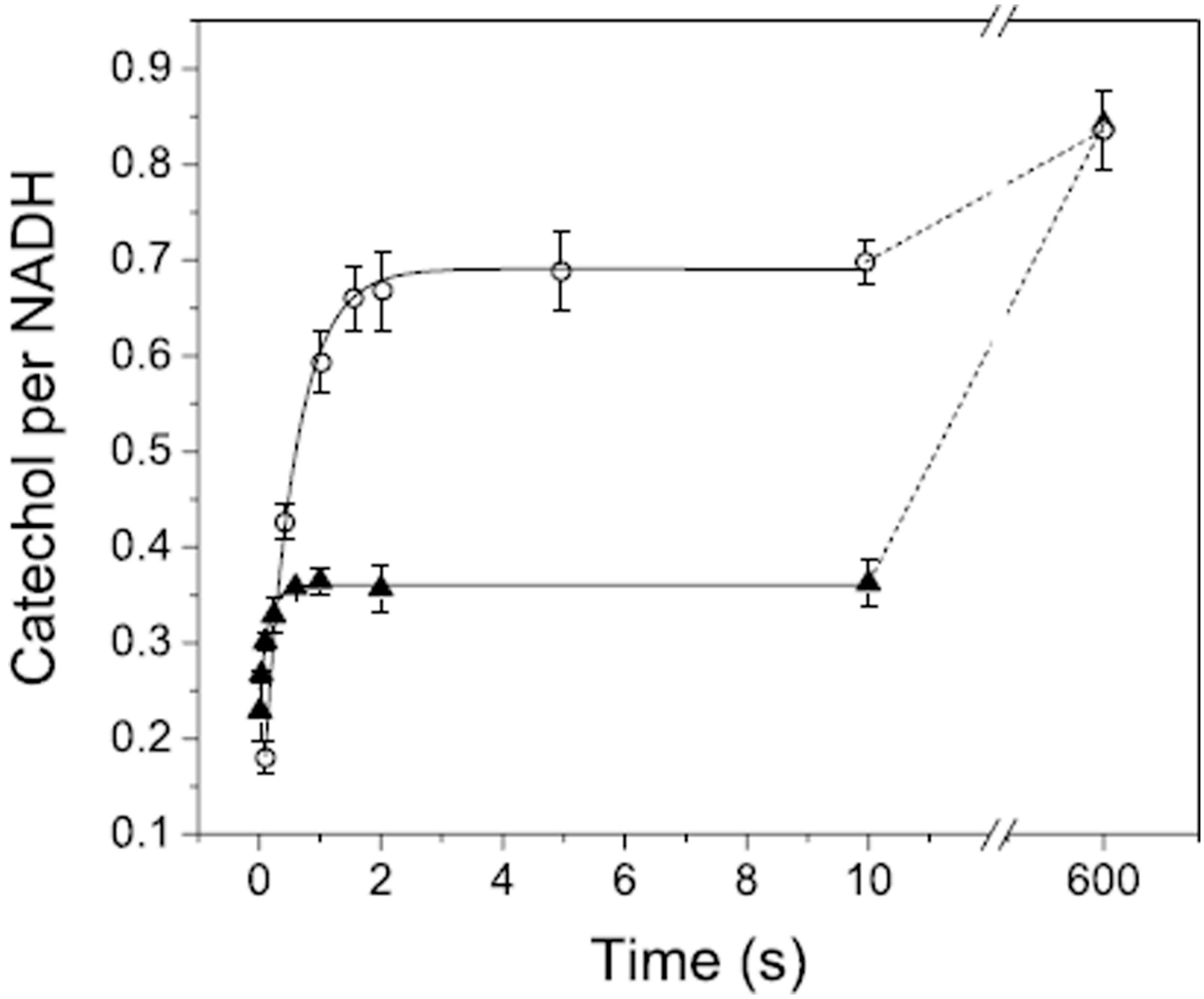

Figure 1.

Hydroxylation of phenol to catechol at 4 °C during single turnover by ToMO. The concentrations of each component are as follows: 50 μM ToMOH (100 μM diiron sites), 100 μM ToMOD, 1 μM (▲) or 100 μM (○) ToMOC, 0.05 μM ToMOF, 90 μM NADH, approximately 625 μM O_2,‡ and 2 mM phenol.

‡O_2–saturated buffer contains ~1.25 mM O_2 at 5 °C. One-to-one mixing yields 625 μM O_2.

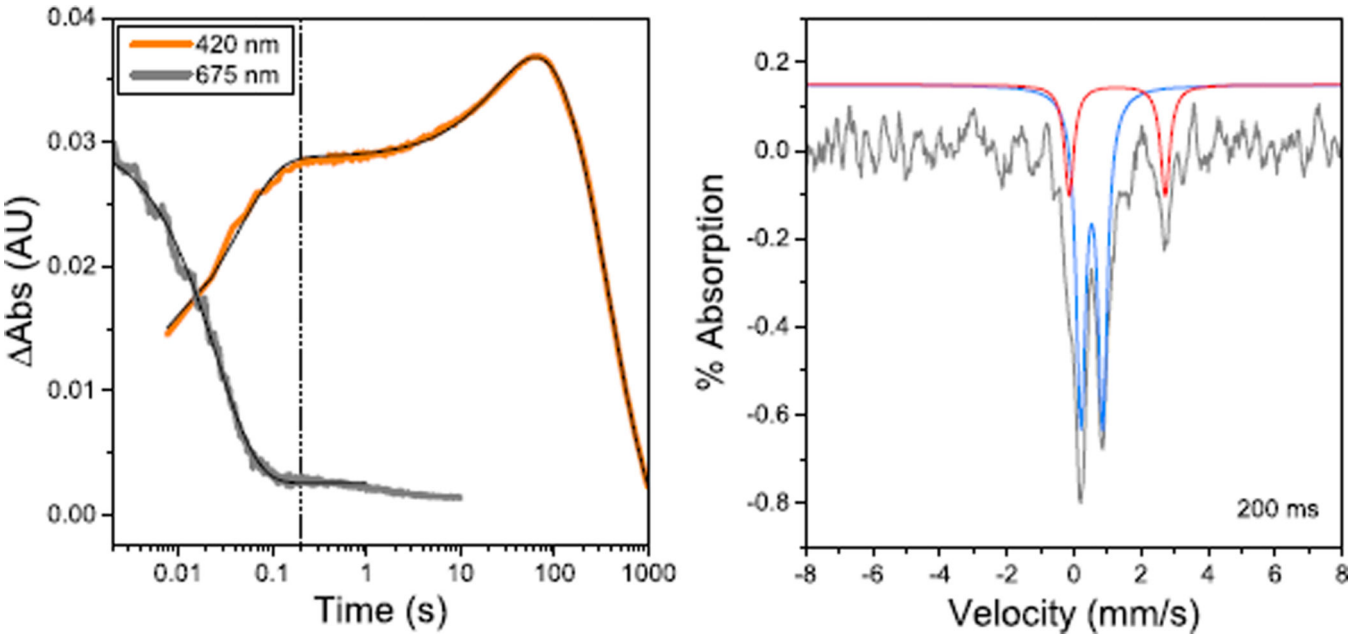

Figure 2.

Analysis of O_2 activation upon mixing of O_2 with $ToMO_{red}$ at 5 °C. *Left*: Time resolved stopped-flow UV-visible spectroscopy of the reaction between $ToMO_{red}$ containing 0.01ToMOC:diiron. The absorbance changes at 420 and 675 nm are shown in orange and grey, respectively. Fits to the absorbance traces are shown in black. *Right*: Mössbauer spectroscopy of the ToMOH diiron site at 0.2 s isolated by rapid freeze-quenching of a reaction containing 0.1ToMOC:diiron. The data were recorded at 80 °C. The Mössbauer signal is shown in grey and the simulated fits in light blue for the Fe^{3+} intermediate (δ = 0.54 mm/s and ΔE_Q = 0.67 mm/s, 80%) and in red for unreacted Fe^{2+} starting material (δ = 1.31 mm/s and ΔE_Q = 2.88 mm/s, 20%).

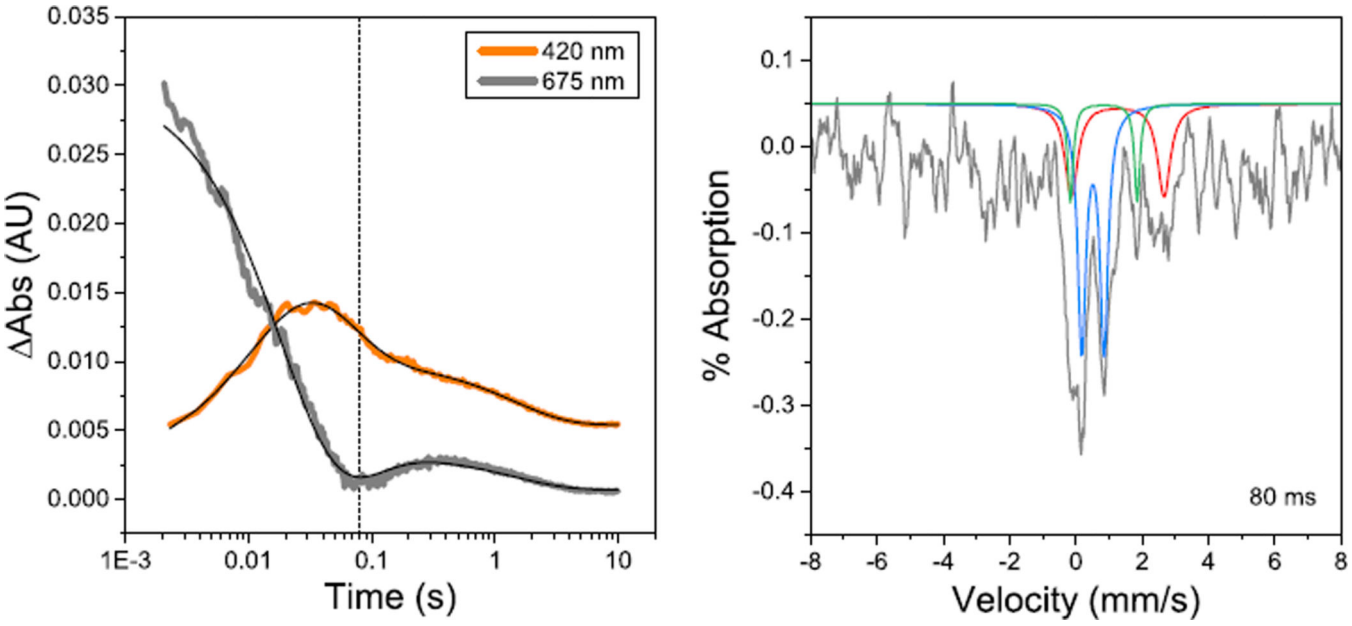

Figure 3.

Analysis of O_2 activation upon mixing of O_2 with $ToMO_{red}$ in the presence of toluene at 5 °C. *Left*: Time resolved stopped-flow UV-visible spectroscopy and ananlysis under the following conditions: 1diiron—1ToMOD—0.01ToMOC—0.0005ToMOF—0.9NADH—20toluene—6.25O_2. The absorbance changes at 420 and 675 nm are shown in orange and grey, respectively. Fits to the absorbance traces are shown in black. *Right*: Analysis of intermediates at 0.2 s by rapid freeze-quench Mössbauer spectroscopy under the following conditions: 1diiron—1ToMOD—0.1ToMOC—0.0005ToMOF—0.9NADH—8toluene—1.25O_2. The Mössbauer signal is shown grey and the simulated species in light blue (δ = 0.52 mm/s and ΔE_Q = 0.67 mm/s, 52%), green (δ = 0.845 mm/s and ΔE_Q = 2.01 mm/s, 27%), and red (δ = 1.26 mm/s and ΔE_Q = 2.79 mm/s, 20%).

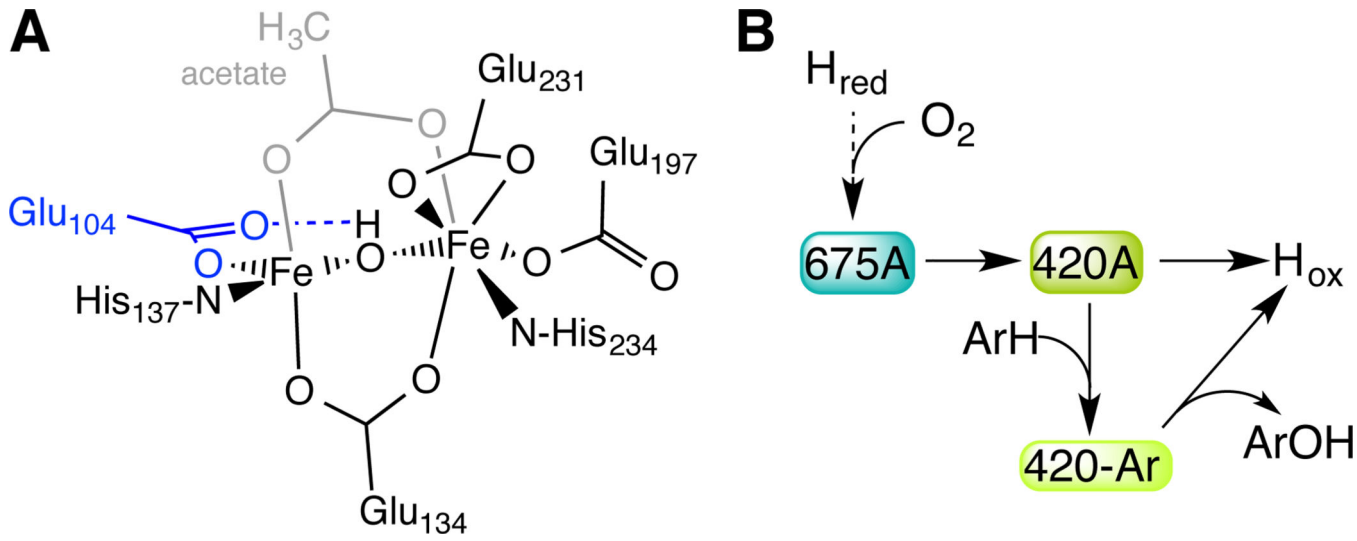

Figure 4.

Influences of ToMOC on the activity of $ToMO_{red}$. Based on the Rieske-hydroxylase complex of T4MO, we propose that an unusual E104 conformation (A) is responsible for the activity seen in the presence of ToMOC. A mechanistic scheme consistent with the activity of $ToMO_{red}$ is provided (B).

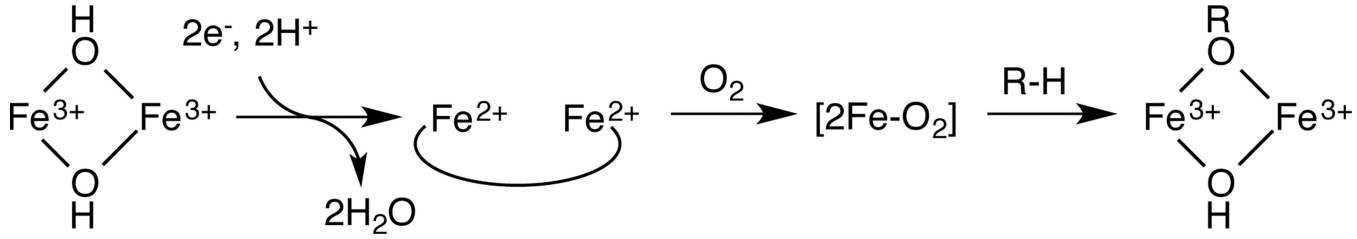

Scheme 1.
General mechanism for hydroxylation by BMMs